Accurate ground-state energies of Wigner crystals from a simple real-space approach

Estefania Alves [1], Gian Luigi Bendazzoli [2], Stefano Evangelisti [3,*] and J. Arjan Berger [4,†]

[1] *CEMES/CNRS, 29 rue J. Marvig, 31055 Toulouse, France*

[2] *Dipartimento di Chimica Industriale, "Toso Montanari", Università di Bologna, Bologna 40126, Italy*

[3] *Laboratoire de Chimie et Physique Quantiques, CNRS, Université de Toulouse, UPS, 118 route de Narbonne, 31062 Toulouse, France*

[4] *Laboratoire de Chimie et Physique Quantiques, CNRS, Université de Toulouse, UPS, and European Theoretical Spectroscopy Facility, 118 route de Narbonne, F-31062 Toulouse, France*

(Received 1 March 2021; revised 21 May 2021; accepted 1 June 2021; published 15 June 2021)

We propose a simple and efficient real-space approach for the calculation of the ground-state energies of Wigner crystals in one, two, and three dimensions. To be precise, we calculate the first two terms in the asymptotic expansion of the total energy per electron which correspond to the classical energy and the harmonic correction due to the zero-point motion of the Wigner crystals. Our approach employs Clifford periodic boundary conditions to simulate the infinite electron gas and a renormalized distance to evaluate the Coulomb potential. This allows us to calculate the energies unambiguously and with a higher precision than those reported in the literature. Our results are in agreement with the literature values with the exception of harmonic correction of the two-dimensional Wigner crystal, for which we find a significant difference. Although we focus on the ground state, i.e., the triangular lattice and the bcc lattice in two and three dimensions, respectively, we also report the classical energies of several other common lattice structures.

DOI: 10.1103/PhysRevB.103.245125

I. INTRODUCTION

The uniform electron gas (UEG) [1,2], otherwise known as jellium, has proven to be a very useful model for the understanding of electron interactions. In particular in the solid state the UEG can be used to study a variety of phenomena, such as plasmon oscillations [3], electron screening [4], the quantum Hall effect [5], and Wigner localization [6–10]. Moreover, by combining the UEG with density-functional theory (DFT) predictive calculations can be performed on both solids and molecules. Thanks to quantum Monte Carlo calculations [11] the correlation contribution to the ground-state energy of the UEG as a function of the density is accurately known. These data have been used to approximate the unknown exchange-correlation energy of DFT [12–14].

Almost a century ago, it was predicted by Wigner [6] that in the limit of an infinitely dilute UEG the electrons crystallize at fixed positions in space, thus forming a crystal lattice. Wigner crystals were later experimentally realized in one and two dimensions and have been shown to exhibit interesting properties [15,16]. However, numerical calculations were required to determine the ground-state crystal structures in both two and three dimensions. By comparing the energies of several Bravais lattices it was concluded that in two dimensions the electrons crystallize in the triangular structure [17], while in three dimensions they crystallize in the bcc structure [6,18–20].

The energy per electron of a Wigner crystal E_{WC} can be written as an asymptotic expansion in powers of $r_s^{-\frac{1}{2}}$ [21]:

$$E_{WC} \sim \frac{\eta_0}{r_s} + \frac{\eta_1}{r_s^{3/2}} + \frac{\eta_2}{r_s^2} + \frac{\eta_3}{r_s^{5/2}} + \cdots , \tag{1}$$

where r_s is the Wigner-Seitz radius. The first term on the right-hand side is the energy corresponding to a classical charge distribution; the second term is a correction due to the zero-point motion in the harmonic approximation, while $\eta_2, \eta_3, \ldots$ correspond to anharmonic corrections. In this work we will focus on the calculation of η_0 and η_1. These parameters have been calculated in the past using reciprocal-space approaches. Here we will show that they can also be calculated within a simple real-space method. We note that Eq. (1) assumes that the electrons are discernible [6]. However, for large r_s the corresponding error is negligible since the correction falls off exponentially with r_s.

For the three-dimensional (3D) Wigner crystal the first accurate calculation of the classical ground-state energy per electron was done by Fuchs and Fowler [18]. They obtained $\eta_0^{3D} = -0.89593$ Ha. This value was later refined to $\eta_0^{3D} = -0.895929$ Ha by Hasse and Avilov [20]. The first estimation of the harmonic correction was done by Wigner, who found $\eta_1^{3D} = 2.7$ Ry [22]. This result is quite close to those obtained two decades later by Coldwell-Horsfall and Maradudin and by Carr; they found $\eta_1^{3D} = 1.319$ Ha [23] and $\eta_1^{3D} = 1.33$ Ha [21], respectively. Using the same approach as Carr but with an improved integration over the Brillouin zone, Nagai and Fukuyama found the most accurate value to date, i.e., $\eta_1^{3D} = 1.32862$ Ha [24].

*stefano.evangelisti@irsamc.ups-tlse.fr

†arjan.berger@irsamc.ups-tlse.fr

TABLE I. Summary of the most accurate literature values (in Ha) of the coefficients η_0 and η_1.

	1D linear lattice	2D triangular lattice	3D bcc lattice
η_0		−1.106 103 [17]	−0.895 929 [20]
η_1	0.359 933 [25]	0.795 [17]	1.328 62 [24]

Both the classical ground-state energy per electron and the harmonic correction of the two-dimensional (2D) Wigner crystal were calculated by Bonsall and Maradudin [17]. They found $\eta_0^{2D} = 1.106103$ Ha and $\eta_1^{2D} = 0.795$ Ha. To the best of our knowledge this is the only calculation of η_1^{2D} in the literature. Below we will show that we obtain a value with much higher precision that differs significantly from the value of Bonsall and Maradudin.

In one dimension the classical ground-state energy per electron diverges because of a nonintegrable singularity in the one-dimensional (1D) Coulomb potential in the origin. Therefore, we will not consider the calculation of η_0^{1D}. We note, however, that regularization techniques can be used for the Coulomb potential to allow for its calculation [25–27]. Instead, η_1^{1D} can be calculated without problems, and its value has been determined with high accuracy [25–27]. Its six-digit approximation is $\eta_1^{1D} = 0.359933$ Ha. In Table I we summarize the most accurate values for η_0 and η_1 that can be found in the literature.

The goal of this work is twofold: (1) to present a simple and general real-space approach for the calculation of the coefficients η_0 and η_1 and (2) to achieve a larger precision of those coefficients, in particular for η_1, for Wigner crystals in two and three dimensions. We will use an approach based on Clifford boundary conditions and a renormalized distance [28] that we previously successfully applied to the calculation of Madelung constants [29,30].

This paper is organized as follows. In Sec. II we describe the theoretical details of our real-space approach. In Sec. III we discuss our results for the energies of the Wigner crystals. Finally, in Sec. IV we draw our conclusions. We use Hartree atomic units ($\hbar = e = m_e = a_0 = 1$) throughout this work.

II. THEORY

A. The jellium model

The Hamiltonian of an infinite uniform electron gas with a uniform positive background that ensures the charge neutrality of the system is given by

$$\hat{H}_{\text{jellium}} = -\sum_i \frac{\nabla_{\vec{r}_i}^2}{2} + \hat{U}_{ee} + \hat{U}_{bb} + \hat{U}_{eb}, \tag{2}$$

in which the electron-electron, electron-background, and background-background contributions to the Coulomb potential are given by, respectively,

$$\hat{U}_{ee} = \frac{1}{2}\sum_{\substack{i,\,j \\ i\neq j}} \frac{1}{|\vec{r}_i - \vec{r}_j|}, \tag{3}$$

$$\hat{U}_{eb} = -\sum_i \int d\vec{r}\,\frac{n}{|\vec{r} - \vec{r}_i|}, \tag{4}$$

$$\hat{U}_{bb} = \frac{1}{2}\int d\vec{r}\int d\vec{r}\,'\,\frac{n^2}{|\vec{r} - \vec{r}\,'|}, \tag{5}$$

where n is the uniform positive background density. The charge neutrality of the system is imposed by assuming that the constant electron density is equal to the positive background density n. Individually, each term in Eq. (2) diverges, but their sum is finite, except for the one-dimensional uniform electron gas.

At low density the electrons form a Wigner crystal with the electrons localized at the lattice positions of a crystal. Therefore, we can perform a Taylor expansion of the Coulomb potential around the equilibrium lattice vectors $\vec{R}$ of the electrons in the Wigner crystal,

$$\hat{H}_{\text{jellium}} = -\frac{1}{2}\sum_i \nabla_{\vec{r}_i}^2 + \hat{U}_0 + \hat{U}_2 + \cdots, \tag{6}$$

in which

$$\hat{U}_0 = \frac{1}{2}\sum_{\substack{i,\,j \\ i\neq j}} \frac{1}{|\vec{R}_i - \vec{R}_j|} - \sum_i \int d\vec{r}\,\frac{n}{|\vec{r} - \vec{R}_i|} + \hat{U}_{bb}, \tag{7}$$

$$\hat{U}_2 = \frac{1}{2}\sum_{mn}\sum_{\alpha\beta} \partial_{m\alpha}\partial_{n\beta}\hat{U}_{ee}|_{\vec{r}_x = \vec{R}_x \forall x} \times (r_{m,\alpha} - R_{m,\alpha})(r_{n,\beta} - R_{n,\beta}), \tag{8}$$

where the Greek letters α and β denote Cartesian components. Since the classical energy U_0 is a minimum, the contribution of the first-order term in the expansion, $\hat{U}_1$, vanishes. Furthermore, only variations in $\hat{U}_{ee}$ contribute to $\hat{U}_2$ since $\hat{U}_{bb}$ is independent of the electronic coordinates and variations in the electronic position do not change $\hat{U}_{be}$ because of the uniformity of the background. In this work we will consider the first three terms on the right-hand side of Eq. (6). This allows us to calculate the first two coefficients in Eq. (1).

Defining the relative coordinates $\vec{u}_m = \vec{r}_m - \vec{R}_m$, we can rewrite the first three terms of Eq. (6) in the following general form [21]:

$$\hat{H} = \hat{U}_0 - \frac{1}{2}\sum_i \nabla_{\vec{u}_i}^2 + \frac{1}{2}\sum_{mn}\sum_{\alpha\beta} C_{\alpha\beta}(\vec{R}_m - \vec{R}_n) u_{m,\alpha} u_{n,\beta}, \tag{9}$$

in which the real symmetric matrix $\mathbf{C}$ is defined as

$$C_{\alpha\beta}(\vec{R}_m - \vec{R}_n) = \frac{1}{2}\partial_{m\alpha}\partial_{n\beta}\sum_{\substack{i,\,j \\ i\neq j}} \frac{1}{|\vec{u}_i - \vec{u}_j + \vec{R}_i - \vec{R}_j|}\bigg|_{\vec{u}_x = 0 \forall x}, \tag{10}$$

where the derivatives are now with respect to $\vec{u}$.

Thanks to the translational invariance of the system we can use the following Fourier transformation:

$$\vec{u}_m = \frac{1}{\sqrt{\mathcal{N}}} \sum_k e^{i\vec{G}_k \cdot \vec{R}_m} \vec{v}_k, \tag{11}$$

$$\vec{v}_k = \frac{1}{\sqrt{\mathcal{N}}} \sum_m e^{-i\vec{G}_k \cdot \vec{R}_m} \vec{u}_m, \tag{12}$$

where $\mathcal{N}$ is a normalization constant and the vectors $\vec{G}_k$ can be interpreted as reciprocal lattice vectors, so Eq. (9) can be rewritten as

$$\hat{H} = \hat{U}_0 + \sum_k \left[-\frac{1}{2} \nabla^2_{\vec{v}_k} + \frac{1}{2} \sum_{\alpha\beta} \tilde{C}_{\alpha\beta}(\vec{G}_k) v_{k,\alpha} v^*_{k,\beta} \right], \tag{13}$$

with

$$\tilde{C}_{\alpha\beta}(\vec{G}_k) = \sum_l C_{\alpha\beta}(\vec{R}_l) e^{i\vec{G}_k \cdot \vec{R}_l} \tag{14}$$

being a real symmetric $d \times d$ matrix, with $d = 1, 2, 3$ being the dimensionality of the lattice. Finally, using the eigenvectors of $C(\vec{G}_k)$, we can perform an orthonormal transformation to arrive at

$$\hat{H} = \hat{U}_0 + \sum_k \sum_\alpha \left[-\frac{1}{2} \partial^2_{k,\alpha} + \frac{1}{2} \omega^2_{k,\alpha} q^2_{k,\alpha} \right], \tag{15}$$

where $\omega^2_{k,\alpha}$ are the eigenvalues of $\tilde{C}(\vec{G}_k)$ and $\vec{q}_k$ are normal modes. The expression inside the square brackets in the above equation is the Hamiltonian of a quantum harmonic oscillator in one dimension for which the eigenenergies are known. Therefore, the total ground-state energy per electron of the Wigner crystal can be written as

$$E_{WC} \sim \frac{\eta_0}{r_s} + \frac{\eta_1}{r_s^{3/2}} + \cdots, \tag{16}$$

with

$$\frac{\eta_0}{r_s} = \frac{U_0}{N}, \tag{17}$$

$$\frac{\eta_1}{r_s^{3/2}} = \frac{1}{2N} \sum_k \sum_\alpha \omega_{k,\alpha}. \tag{18}$$

The jellium problem pertains to a system with an infinite number of electrons in an infinite volume at constant density. In practical calculations we can, of course, deal with only a finite number of electrons in a finite volume. However, we would like to preserve the translational symmetry of the jellium model. Therefore, we impose periodic boundary conditions (PBC) with respect to a finite supercell. Unfortunately, the long-range Coulomb potential is not periodic, and it does not vanish at the borders of any finite supercell, even a very large one. Therefore, as explained in the next section, we impose Clifford boundary conditions with a renormalized distance.

B. Clifford boundary conditions

We will use Clifford boundary conditions, which means that we define a supercell that has the topology of a Clifford torus, i.e., a finite, flat, and borderless manifold. A Clifford supercell is linked to a Euclidean supercell defined in $\mathbb{R}^d$. The Clifford supercell is then obtained by joining opposite sides of the Euclidean supercell *without* deformation. This can be achieved by defining the Clifford supercell in the embedding space $\mathbb{C}^d$ (alternatively, it can also be achieved in $\mathbb{R}^{2d}$).

Let us consider a general orthorhombic lattice in d dimensions and define $\vec{a}_\alpha$ to be the orthogonal generating vectors of a unit cell in $\mathbb{R}^d$. Then a general vector $\vec{v}$ inside the unit cell can be written as

$$\vec{v} = \sum_\alpha x_\alpha \vec{a}_\alpha, \tag{19}$$

where $0 \leqslant x_\alpha < 1$. We define a Euclidean supercell (ESC) as the right parallelepiped in $\mathbb{R}^d$ generated by the vectors $\vec{A}_\alpha$ given by

$$\vec{A}_\alpha = K_\alpha \vec{a}_\alpha, \tag{20}$$

where K_α are positive integers. The ESC thus contains $\prod_\alpha K_\alpha$ copies of the unit cell. A general vector $\vec{r}^{\,\mathrm{ESC}}$ in the ESC can thus be written as

$$\vec{r}^{\,\mathrm{ESC}} = \vec{v} + \sum_\alpha k_\alpha \vec{a}_\alpha = \sum_\alpha r_\alpha \vec{a}_\alpha, \tag{21}$$

with $r_\alpha = x_\alpha + k_\alpha$ and $0 \leqslant k_\alpha \leqslant K_\alpha - 1$.

We now define the Clifford supercell (CSC) as the Clifford torus in which the opposite borders (either points, edges, or faces, depending on d) of the corresponding ESC are connected without deformation. A general vector $\vec{r}^{\,\mathrm{CSC}}$ in the CSC should respect the translational symmetry of the Clifford torus. This can be achieved by writing $\vec{r}^{\,\mathrm{CSC}}$ according to

$$\vec{r}^{\,\mathrm{CSC}} = \sum_\alpha \frac{K_\alpha}{2\pi i} [e^{i2\pi r_\alpha / K_\alpha} - 1] \vec{a}_\alpha. \tag{22}$$

We note that the above expression is the classical equivalent of the PBC position operator proposed by some of us in a quantum context [28]. The above definition satisfies a number of important constraints. In particular, it satisfies the translational symmetry, it reduces to the standard position operator in the appropriate limit, and the corresponding definition of the distance is real and gauge invariant [see Eq. (23)] [28].

In order to evaluate Coulomb potentials we have to define the distance between two points in the CSC. We note that a possibility would be to define the distance as the smallest difference between two points *on* the Clifford torus. However, such a distance would have discontinuous derivatives in those points of the CSC that correspond to the midpoints of the edges of the corresponding ESC. This definition of the distance would yield discontinuous forces in these points, which is unphysical. Therefore, we choose the distance to be the Euclidean norm in $\mathbb{C}^d$ because it is both uniquely defined and yields continuous derivatives. In other words, the distance is defined in the embedding space of the Clifford torus. This distance $r_{ij}^{\mathrm{CSC}} = |\vec{r}_i^{\,\mathrm{CSC}} - \vec{r}_j^{\,\mathrm{CSC}}|$ is given by

$$r_{ij}^{\mathrm{CSC}} = \sqrt{\sum_\alpha \frac{L_\alpha^2}{\pi^2} \sin^2 \left(\frac{\pi}{L_\alpha} [r_{i\alpha} - r_{j\alpha}] \right)}, \tag{23}$$

where we used $\vec{a}_\alpha \cdot \vec{a}_\beta = 0$ for $\alpha \neq \beta$ and $L_\alpha = K_\alpha |\vec{a}_\alpha|$, with L_α being the length of an edge of the ESC. We will evaluate the Coulomb potentials in Eqs. (7) and (8) using the above renormalized distance. In Fig. 1 we show an illustration of a

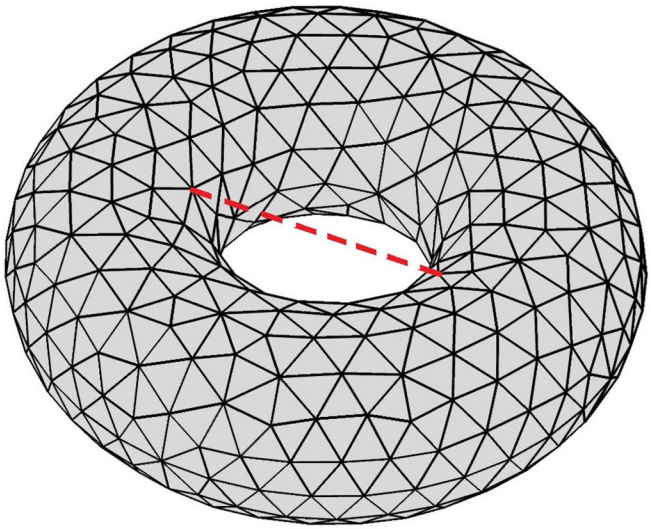

FIG. 1. Pictorial illustration of a Clifford supercell for the triangular lattice of the two-dimensional Wigner crystal. The equilibrium positions of the electrons are located at the vertices. The dashed red line represents the renormalized distance between two electrons used in the Coulomb potential. It is the shortest distance in the embedding space of the Clifford torus. We note that a true Clifford torus has a flat surface which is impossible to represent graphically.

CSC for a two-dimensional Wigner crystal and the renormalized distance between the electrons.

C. The 3D Wigner crystal

With the renormalized distance the background-background contribution in the 3D CSC is given by

$$\hat{U}_{bb}^{\mathrm{CSC}} = \frac{N^2}{2V}\int_V \frac{dx\,dy\,dz}{\sqrt{\frac{L_x^2}{\pi^2}\sin^2\left[\frac{\pi x}{L_x}\right]+\frac{L_y^2}{\pi^2}\sin^2\left[\frac{\pi y}{L_y}\right]+\frac{L_z^2}{\pi^2}\sin^2\left[\frac{\pi z}{L_z}\right]}}, \tag{24}$$

where, thanks to the periodicity of the CSC, we could reduce the two volume integrals to only one and we used $n = N/V$, which ensures the charge neutrality of the 3D CSC supercell, with $V = L_x L_y L_z$ being the volume of the supercell. With the changes in variable $\theta_x = \frac{\pi x}{L}$, $\theta_y = \frac{\pi y}{L}$, and $\theta_z = \frac{\pi z}{L}$ the above expression can be rewritten according to

$$\hat{U}_{bb}^{\mathrm{CSC}} = \frac{N^2}{2\pi^2}\int_0^\pi\int_0^\pi\int_0^\pi \frac{d\theta_x d\theta_y d\theta_z}{\sqrt{L_x^2\sin^2\theta_x + L_y^2\sin^2\theta_y + L_z^2\sin^2\theta_z}}. \tag{25}$$

The triple integral in the above equation can be readily calculated. For example, in the case of a cubic supercell, i.e., $L = L_x = L_y = L_z$, we obtain the following result:

$$\hat{U}_{bb}^{\mathrm{CSC}} = \frac{N^2\gamma_c}{L} \quad (L = L_x = L_y = L_z), \tag{26}$$

with $\gamma_c = 1.4305055275$.

Thanks to the periodicity and uniformity of the positive background, each electron contributes exactly the same amount to the summation in the expression of the electron-background contribution in the CSC. Therefore, without loss of generality, we can choose to consider explicitly only the contribution of an electron located at the origin and multiply by N. We can thus write the electron-background contribution according to

$$\hat{U}_{eb}^{\mathrm{CSC}} = -\frac{N^2}{V}\int_V \frac{dx\,dy\,dz}{\sqrt{\frac{L_x^2}{\pi^2}\sin^2\left[\frac{\pi x}{L_x}\right]+\frac{L_y^2}{\pi^2}\sin^2\left[\frac{\pi y}{L_y}\right]+\frac{L_z^2}{\pi^2}\sin^2\left[\frac{\pi z}{L_z}\right]}}, \tag{27}$$

where we once more used $n = N/V$. We note that in the special case $L = L_x = L_y = L_z$ the integral in the above equation can be made independent of L in a way similar to what was done for $\hat{U}_{bb}$. By comparing Eqs. (24) and (27) we find the following identity between $\hat{U}_{bb}$ and $\hat{U}_{eb}$ in the CSC:

$$\hat{U}_{eb}^{\mathrm{CSC}} = -2\hat{U}_{bb}^{\mathrm{CSC}}. \tag{28}$$

Finally, the classical electron-electron contribution $\hat{U}_{0,ee}$ in the CSC is given by

$$\hat{U}_{0,ee}^{\mathrm{CSC}} = \frac{1}{2}\sum_{\substack{i,\,j\\ i\neq j}} \frac{1}{\sqrt{\frac{L_x^2}{\pi^2}\sin^2\left[\frac{\pi}{L_x}(x_i-x_j)\right]+\frac{L_y^2}{\pi^2}\sin^2\left[\frac{\pi}{L_y}(y_i-y_j)\right]+\frac{L_z^2}{\pi^2}\sin^2\left[\frac{\pi}{L_z}(z_i-z_j)\right]}}. \tag{29}$$

This is the only contribution that depends on the details of the lattice structure, i.e., the equilibrium positions of the electrons.

In the following we will focus on the bcc lattice since it yields the ground-state energy of a 3D Wigner crystal. A strategy similar to that described below can be used for other lattices. For the bcc structure it is convenient to use a cubic supercell, i.e., $L = L_x = L_y = L_z$, and to define the equilibrium positions of the electrons according to $\vec{R}_i = (\pi/3)^{1/3} r_s \vec{n}_i$, with $\vec{n}_i$ being a vector of three integers, all even or all odd [21]. Therefore, $L = (\pi/3)^{1/3}(2N_s)r_s$, with N_s being the number of electrons per side. The total classical bcc energy $U_0 = U_{0,ee}^{\mathrm{CSC}} - U_{bb}^{\mathrm{CSC}}$ per electron can thus be written as

$$\frac{U_0}{N} = \frac{\left(\frac{3}{\pi}\right)^{1/3}}{2N_s r_s}\left\{\frac{\pi}{2}\sum_{i=1}^{N}\left(\sum_\alpha \sin^2\left[\frac{\pi n_{i\alpha}}{2N_s}\right]\right)^{-1/2} - \gamma_c N\right\}. \tag{30}$$

Since $U_0/N = \eta_0^{bcc}/r_s$, we can easily obtain η_0^{bcc} from the above expression.

By working out the derivatives in Eq. (10) while using the renormalized distance given in Eq. (23) and then inserting

the definition of $\vec{R}_i$ for the bcc lattice, i.e., $\vec{R}_i = (\pi/3)^{1/3} r_s \vec{n}_i$, we obtain the following expression for the **C** matrix:

$$C^{N_s}_{\alpha\beta}(\vec{0}) = -\frac{3\pi^2}{8N_s^3}\frac{\delta_{\alpha\beta}}{r_s^3}\sum_{\vec{n}_i\neq\vec{0}}\left[\frac{\cos\left[\frac{\pi n_{i\alpha}}{N_s}\right]}{\left\{\sum_{\alpha'}\sin^2[\pi n_{i\alpha'}/(2N_s)]\right\}^{3/2}} - \frac{\frac{3}{4}\sin^2\left[\frac{\pi n_{i\alpha}}{N_s}\right]}{\left\{\sum_{\alpha'}\sin^2[\pi n_{i\alpha'}/(2N_s)]\right\}^{5/2}}\right], \tag{31}$$

$$C^{N_s}_{\alpha\beta}(\vec{n}_i) = \frac{3\pi^2}{8N_s^3}\frac{1}{r_s^3}\left[\frac{\delta_{\alpha\beta}\cos\left[\frac{\pi n_{i\alpha}}{N_s}\right]}{\sum_{\alpha'}\{\sin^2[\pi n_{i\alpha'}/(2N_s)]\}^{3/2}} - \frac{\frac{3}{4}\sin\left[\frac{\pi n_{i\alpha}}{N_s}\right]\sin[\frac{\pi n_{i\beta}}{N_s}]}{\sum_{\alpha'}\{\sin^2[\pi n_{i\alpha'}/(2N_s)]\}^{5/2}}\right] \quad (\vec{n}_i \neq \vec{0}), \tag{32}$$

where the summation in Eq. (31) is over all $\vec{n}_i \neq \vec{0}$ inside the CSC. We note that in the limit $N_s \to \infty$ we have the following identity:

$$\lim_{N_s\to\infty} C^{N_s}_{\alpha\alpha}(\vec{0}) = \frac{1}{r_s^3}. \tag{33}$$

The matrix $\tilde{\mathbf{C}}$ given in Eq. (14) can be rewritten as

$$\tilde{\mathbf{C}}^{N_s}(\vec{n}_k) = \sum_{\vec{n}_i}\mathbf{C}^{N_s}(\vec{n}_i)\cos\left(\frac{\pi\vec{n}_k\cdot\vec{n}_i}{N_s}\right), \tag{34}$$

where we used that $\vec{G}_k = 2\pi\vec{n}_k/(2N_s)$. To obtain η_1^{bcc} it suffices to diagonalize $\tilde{\mathbf{C}}^{N_s}(\vec{n}_k)\,\forall\, k$, take the square root of the eigenvalues, and add them up according to Eq. (18).

D. The 2D Wigner crystal

The derivation of the various terms of the Coulomb potential in two dimensions for the CSC are analogous to those of the 3D Wigner crystal discussed in the previous section. The background-background and electron-background contributions in the CSC are given by

$$\hat{U}^{\rm CSC}_{bb} = -\frac{\hat{U}_{eb}}{2} = \frac{N^2}{2\pi}\int_0^\pi\int_0^\pi \frac{d\theta_x d\theta_y}{\sqrt{L_x^2\sin^2\theta_x + L_y^2\sin^2\theta_y}}, \tag{35}$$

where we used the fact that in 2D $n = N/(L_xL_y)$. We note that in the special case $L = L_x = L_y$ we obtain the following analytical expression:

$$\hat{U}^{\rm CSC}_{bb} = -\frac{\hat{U}_{eb}}{2} = \frac{N^2}{2\sqrt{\pi}L}G^{2,2}_{3,3}\left(\begin{matrix}1,1,1\\1/2,1/2,1/2\end{matrix}\middle|1\right), \tag{36}$$

where G is the Meijer G function. The classical electron-electron contribution in the 2D CSC is given by

$$\hat{U}^{\rm CSC}_{0,ee} = \frac{1}{2}\sum_{\substack{i,\,j\\ i\neq j}}\frac{1}{\sqrt{\frac{L_x^2}{\pi^2}\sin^2\left[\frac{\pi}{L_x}(x_i-x_j)\right] + \frac{L_y^2}{\pi^2}\sin^2\left[\frac{\pi}{L_y}(y_i-y_j)\right]}}. \tag{37}$$

In the following we will focus on the triangular lattice since it yields the ground-state energy of a 2D Wigner crystal. For the triangular lattice it is convenient to use a rectangular supercell and to define the equilibrium positions of the electrons according to $\vec{R}_i = r_s\sqrt{\pi/(2\sqrt{3})}(n_{ix}, n_{iy}\sqrt{3})^T$, with n_x and n_y being two integers, both even or both odd. Therefore, $L_x = r_s\sqrt{2\pi/\sqrt{3}}N_s$, and $L_y = r_s\sqrt{2\pi\sqrt{3}}N_s$. The total classical energy $U_0 = U^{\rm CSC}_{0,ee} - U^{\rm CSC}_{bb}$ per electron of the triangular lattice can thus be written as

$$\frac{U_0}{N} = \frac{1}{N_s r_s}\left[\frac{\sqrt{\pi}}{2\sqrt{2}}\sum_{i=1}^{N}\frac{3^{1/4}}{\sqrt{f(\vec{n}_i)}} - \gamma_t N\right], \tag{38}$$

where $\gamma_t = 0.7839363355$ and

$$f(\vec{n}_i) = \sin^2\left[\frac{\pi n_{ix}}{2N_s}\right] + 3\sin^2\left[\frac{\pi n_{iy}}{2N_s}\right]. \tag{39}$$

By working out the derivatives in Eq. (10) while using the renormalized distance given in Eq. (23) and then inserting the definition of $\vec{R}_i$ for the triangular lattice, i.e., $\vec{R}_i = r_s\sqrt{\pi/(2\sqrt{3})}(n_x, n_y\sqrt{3})^T$, we obtain the following expression for the **C** matrix:

$$C^{N_s}_{\alpha\beta}(\vec{0}) = -\left(\frac{\pi\sqrt{3}}{2N_s^2}\right)^{3/2}\frac{\delta_{\alpha\beta}}{r_s^3}\sum_{\vec{n}_i\neq\vec{0}}\left[\frac{\cos\left[\frac{\pi n_{i\alpha}}{N_s}\right]}{f(\vec{n}_i)^{3/2}} - \frac{\frac{3}{4}(\sqrt{3})^{\delta_{\alpha y}}(\sqrt{3})^{\delta_{\beta y}}\sin^2\left[\frac{\pi n_{i\alpha}}{N_s}\right]}{f(\vec{n}_i)^{5/2}}\right], \tag{40}$$

$$C^{N_s}_{\alpha\beta}(\vec{n}_i) = \left(\frac{\pi\sqrt{3}}{2N_s^2}\right)^{3/2}\frac{1}{r_s^3}\left[\frac{\delta_{\alpha\beta}\cos\left[\frac{\pi n_{i\alpha}}{N_s}\right]}{f(\vec{n}_i)^{3/2}} - \frac{\frac{3}{4}(\sqrt{3})^{\delta_{\alpha y}}(\sqrt{3})^{\delta_{\beta y}}\sin\left[\frac{\pi n_{i\alpha}}{N_s}\right]\sin\left[\frac{\pi n_{i\beta}}{N_s}\right]}{f(\vec{n}_i)^{5/2}}\right] \quad (\vec{n}_i \neq \vec{0}), \tag{41}$$

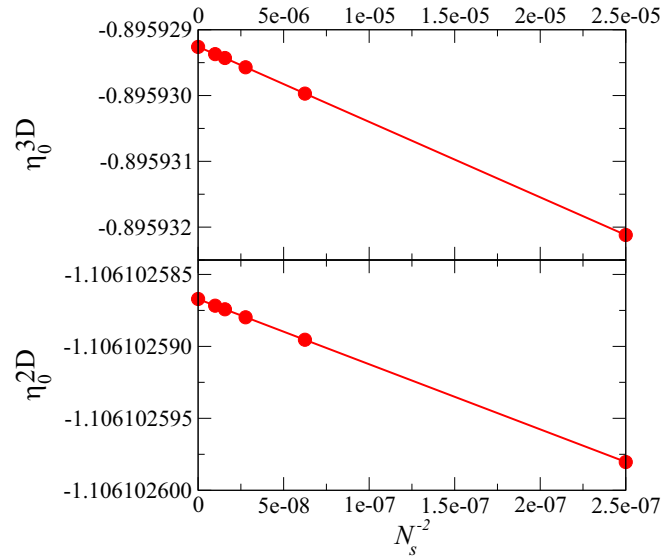

FIG. 2. The coefficient η_0 (in Ha) as a function of N_s^{-2} for the 3D bcc lattice and the 2D triangular lattice. The dots at $N_s^{-2} = 0$ indicate the extrapolated values obtained according to Eq. (45).

TABLE II. Numerical values of η_0^{2D} (in Ha) for the square and triangular 2D crystal structures.

	η_0^{2D}	
Lattice	This work	Literature [17]
Square	−1.100244420	−1.100 244
Triangle	−1.106 102 587	−1.106 103

where the summation in Eq. (40) is over all $\vec{n}_i \neq \vec{0}$ inside the CSC. A procedure similar to that described for the 3D bcc lattice in the previous section then leads to η_1^{2D}.

E. The 1D Wigner crystal

As mentioned in the Introduction, in one dimension the classical ground-state energy per electron diverges because of a nonintegrable singularity in the 1D Coulomb potential. Therefore, we will focus here on the calculation of η_1. In one dimension the C matrix defined in Eq. (10) is just a scalar that is given by

$$C^N(0) = \frac{\pi^3}{8N^3}\frac{1}{r_s^3}\sum_{n=1}^{N-1}\frac{1+\cos^2[\pi n/N]}{|\sin[\pi n/N]|^3}, \tag{42}$$

$$C^N(n) = -\frac{\pi^3}{8N^3}\frac{1}{r_s^3}\frac{1+\cos^2[\pi n/N]}{|\sin[\pi n/N]|^3} \quad (n \neq 0). \tag{43}$$

We note that in the limit $N \to \infty$ we have the following identity:

$$\lim_{N\to\infty} C^N(0) = \frac{\zeta(3)}{2r_s^3} \tag{44}$$

in terms of the Riemann ζ function.

III. RESULTS

We summarize here the results obtained for η_0 and η_1 for various lattices in the limit of the infinite systems. To estimate the coefficients η_0 and η_1 for the infinite CSC we extrapolate the coefficients of finite-size CSCs with the following power function:

$$\eta(N_s) = \eta_\infty + AN_s^{-2}, \tag{45}$$

where A and η_∞ are the fit coefficients. This power function has also proven to work well for the extrapolation of Madelung constants [29].

TABLE III. Numerical values of η_0^{3D} (in Ha) for several 3D crystal structures.

	η_0^{3D}	
Lattice	This work	Literature [20]
Simple cubic	−0.880 059 440	−0.880 059
bcc	−0.895 929 255	−0.895 929
fcc	−0.895 873 614	−0.895 874
hcp	−0.895 838 120	−0.895 838

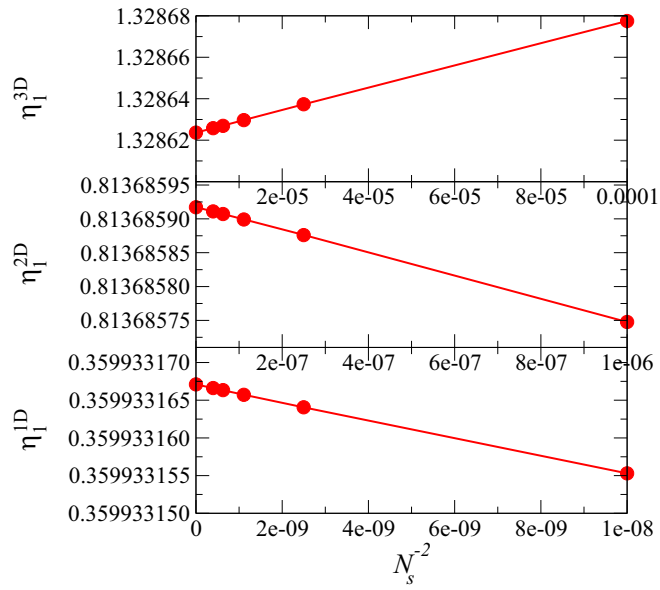

FIG. 3. The coefficient η_1 (in Ha) as a function of N_s^{-2} for the 3D bcc lattice, the 2D triangular lattice, and the 1D linear lattice. The dots at $N_s^{-2} = 0$ indicate the extrapolated values obtained according to Eq. (45).

A. The classical energy η_0

In Fig. 2 we report η_0^{3D} and η_0^{2D} as a function of N_s^{-2} for the bcc and triangular lattices, respectively.

We can use the same strategy to find the ground-state energy for any crystal structure. For the sake of completeness we report in Tables II and III the ground-state energies of the most common crystal structures in two and three dimensions, respectively. As expected, we find that in two dimensions the triangular lattice is lower in energy than the square lattice, while in three dimensions, it is the bcc lattice that has the lowest energy, although the differences from the fcc and hcp lattices are small. Our results are in perfect agreement with the literature values, while with our approach we can easily obtain several more digits.

B. The harmonic correction, η_1

In Fig. 3 we report η_1 as a function of N_s^{-2} for one, two, and three dimensions. Again, the results are close to linear, and we can extrapolate to the infinite-size CSC with the power function of Eq. (45). We report the extrapolated values in Table IV. We see that for the 1D and 3D Wigner crystals our results are in agreement with the most accurate values found in the literature. Instead, for the triangular 2D Wigner crystal our result is significantly different from the literature value.

TABLE IV. Numerical values of η_1 (in Ha) for Wigner crystals in one, two, and three dimensions.

	η_1	
Lattice	This work	Literature
1D (linear)	0.359 933	0.359 933 [25]
2D (triangular)	0.813 686	0.795 [17]
3D (bcc)	1.328 624	1.328 62 [21]

TABLE V. Summary of the coefficients η_0 and η_1 (in Ha) obtained in this work.

	1D linear lattice	2D triangular lattice	3D bcc lattice
η_0		−1.106 103	−0.895 929
η_1	0.359 933	0.813 686	1.328 624

IV. CONCLUSIONS

We have presented a simple real-space approach for the calculation of the ground-state energy of Wigner crystals in one, two, and three dimensions. Our approach yields values with high precision for the first two terms in the asymptotic expansion of the energy per electron of Wigner crystals. Our results are in agreement with the values found in the literature with the exception of the harmonic correction to the zero-point energy of the 2D triangular Wigner crystal, for which we found a significantly larger value than the one in the literature. We summarize our results in Table V. Finally, we note that all our results were obtained with simple computer codes of no more than a few hundred lines, all of which are freely available [31].

ACKNOWLEDGMENTS

J.A.B. thanks the French Agence Nationale de la Recherche (ANR) for financial support (Grant Agreement ANR-19-CE30-0011).

[1] G. F. Giuliani and G. Vignale, *Quantum Theory of the Electron Liquid* (Cambridge University Press, Cambridge, 2005).
[2] P.-F. Loos and P. M. W. Gill, The uniform electron gas, Wiley Interdiscip. Rev.: Comput. Mol. Sci. **6**, 410 (2016).
[3] L. Tonks and I. Langmuir, Oscillations in ionized gases, Phys. Rev. **33**, 195 (1929).
[4] J. Lindhard, On the properties of a gas of charged particles, K. Dan. Vidensk. Selsk., Mat.-Fys. Skr. **28**, 1 (1954).
[5] K. V. Klitzing, G. Dorda, and M. Pepper, New Method for High-Accuracy Determination of the Fine-Structure Constant Based on Quantized Hall Resistance, Phys. Rev. Lett. **45**, 494 (1980).
[6] E. Wigner, On the interaction of electrons in metals, Phys. Rev. **46**, 1002 (1934).
[7] K. Jauregui, W. Häusler, and B. Kramer, Wigner molecules in nanostructures, Europhys. Lett. **24**, 581 (1993).
[8] A. Diaz-Marquez, S. Battaglia, G. L. Bendazzoli, S. Evangelisti, T. Leininger, and J. A. Berger, Signatures of Wigner localization in one-dimensional systems, J. Chem. Phys. **148**, 124103 (2018).
[9] M. Escobar Azor, L. Brooke, S. Evangelisti, T. Leininger, P.-F. Loos, N. Suaud, and J. A. Berger, A Wigner molecule at extremely low densities: A numerically exact study, SciPost Phys. Core **1**, 001 (2019).
[10] N. T. Ziani, F. Cavaliere, K. G. Becerra, and M. Sassetti, A short review of one-dimensional Wigner crystallization, Crystals **11**, 20 (2021).
[11] D. M. Ceperley and B. J. Alder, Ground State of the Electron Gas by a Stochastic Method, Phys. Rev. Lett. **45**, 566 (1980).
[12] S. H. Vosko, L. Wilk, and M. Nusair, Accurate spin-dependent electron liquid correlation energies for local spin density calculations: A critical analysis, Can. J. Phys. **58**, 1200 (1980).
[13] J. P. Perdew and A. Zunger, Self-interaction correction to density-functional approximations for many-electron systems, Phys. Rev. B **23**, 5048 (1981).
[14] J. P. Perdew and Y. Wang, Accurate and simple analytic representation of the electron-gas correlation energy, Phys. Rev. B **45**, 13244 (1992).
[15] I. Shapir, A. Hamo, S. Pecker, C. P. Moca, Ö. Legeza, G. Zarand, and S. Ilani, Imaging the electronic Wigner crystal in one dimension, Science **364**, 870 (2019).
[16] C. C. Grimes and G. Adams, Evidence for a Liquid-to-Crystal Phase Transition in a Classical, Two-Dimensional Sheet of Electrons, Phys. Rev. Lett. **42**, 795 (1979).
[17] L. Bonsall and A. A. Maradudin, Some static and dynamical properties of a two-dimensional Wigner crystal, Phys. Rev. B **15**, 1959 (1977).
[18] K. Fuchs and R. H. Fowler, A quantum mechanical investigation of the cohesive forces of metallic copper, Proc. R. Soc. London, Ser. A **151**, 585 (1935).
[19] C. A. Sholl, The calculation of electrostatic energies of metals by plane-wise summation, Proc. Phys. Soc. **92**, 434 (1967).
[20] R. W. Hasse and V. V. Avilov, Structure and Madelung energy of spherical Coulomb crystals, Phys. Rev. A **44**, 4506 (1991).
[21] W. J. Carr, Energy, specific heat, and magnetic properties of the low-density electron gas, Phys. Rev. **122**, 1437 (1961).
[22] E. Wigner, Effects of the electron interaction on the energy levels of electrons in metals, Trans. Faraday Soc. **34**, 678 (1938).
[23] R. A. Coldwell-Horsfall and A. A. Maradudin, Zero-point energy of an electron lattice, J. Math. Phys. **1**, 395 (1960).
[24] T. Nagai and H. Fukuyama, Ground state of a Wigner crystal in a magnetic field I. Cubic structure, J. Phys. Soc. Jpn. **51**, 3431 (1982).
[25] M. M. Fogler, Ground-State Energy of the Electron Liquid in Ultrathin Wires, Phys. Rev. Lett. **94**, 056405 (2005).
[26] P.-F. Loos and P. M. W. Gill, Uniform electron gases. I. Electrons on a ring, J. Chem. Phys. **138**, 164124 (2013).
[27] P.-F. Loos, Generalized local-density approximation and one-dimensional finite uniform electron gases, Phys. Rev. A **89**, 052523 (2014).
[28] E. Valença Ferreira de Aragão, D. Moreno, S. Battaglia, G. L. Bendazzoli, S. Evangelisti, T. Leininger, N. Suaud, and J. A. Berger, A simple position operator for periodic systems, Phys. Rev. B **99**, 205144 (2019).
[29] N. Tavernier, G. L. Bendazzoli, V. Brumas, S. Evangelisti, and J. A. Berger, Clifford boundary conditions: A simple direct-sum evaluation of Madelung constants, J. Phys. Chem. Lett. **11**, 7090 (2020).
[30] N. Tavernier, G. L. Bendazzoli, V. Brumas, S. Evangelisti, and J. A. Berger, Clifford boundary conditions for periodic systems: The Madelung constant of cubic crystals in 1, 2 and 3 dimensions (unpublished).
[31] https://git.irsamc.ups-tlse.fr/berger/Wigner.